Study of e^{+}e^{-}→ωχ_{cJ} at Center of Mass Energies from 4.21 to 4.42 GeV

M. Ablikim *et al.* (BESIII Collaboration)

Study of $e^+e^- \to \omega\chi_{cJ}$ at center-of-mass energies from 4.21 to 4.42 GeV

M. Ablikim[1], M. N. Achasov[8,a], X. C. Ai[1], O. Albayrak[4], M. Albrecht[3], D. J. Ambrose[42], A. Amoroso[46A,46C], F. F. An[1], Q. An[43], J. Z. Bai[1], R. Baldini Ferroli[19A], Y. Ban[30], D. W. Bennett[18], J. V. Bennett[4], M. Bertani[19A], D. Bettoni[20A], J. M. Bian[41], F. Bianchi[46A,46C], E. Boger[22,g], O. Bondarenko[24], I. Boyko[22], R. A. Briere[4], H. Cai[48], X. Cai[1], O. Cakir[38A], A. Calcaterra[19A], G. F. Cao[1], S. A. Cetin[38B], J. F. Chang[1], G. Chelkov[22,b], G. Chen[1], H. S. Chen[1], H. Y. Chen[2], J. C. Chen[1], M. L. Chen[1], S. J. Chen[28], X. Chen[1], X. R. Chen[25], Y. B. Chen[1], H. P. Cheng[16], X. K. Chu[30], Y. P. Chu[1], G. Cibinetto[20A], D. Cronin-Hennessy[41], H. L. Dai[1], J. P. Dai[1], D. Dedovich[22], Z. Y. Deng[1], A. Denig[21], I. Denysenko[22], M. Destefanis[46A,46C], F. De Mori[46A,46C], Y. Ding[26], C. Dong[29], J. Dong[1], L. Y. Dong[1], M. Y. Dong[1], S. X. Du[50], P. F. Duan[1], J. Z. Fan[37], J. Fang[1], S. S. Fang[1], X. Fang[43], Y. Fang[1], L. Fava[46B,46C], F. Feldbauer[21], G. Felici[19A], C. Q. Feng[43], E. Fioravanti[20A], C. D. Fu[1], Q. Gao[1], Y. Gao[37], I. Garzia[20A], K. Goetzen[9], W. X. Gong[1], W. Gradl[21], M. Greco[46A,46C], M. H. Gu[1], Y. T. Gu[11], Y. H. Guan[1], A. Q. Guo[1], L. B. Guo[27], T. Guo[27], Y. Guo[1], Y. P. Guo[21], Z. Haddadi[24], A. Hafner[21], S. Han[48], Y. L. Han[1], F. A. Harris[40], K. L. He[1], Z. Y. He[29], T. Held[3], Y. K. Heng[1], Z. L. Hou[1], C. Hu[27], H. M. Hu[1], J. F. Hu[46A], T. Hu[1], Y. Hu[1], G. M. Huang[5], G. S. Huang[43], H. P. Huang[48], J. S. Huang[14], X. T. Huang[32], Y. Huang[28], T. Hussain[45], Q. Ji[1], Q. P. Ji[29], X. B. Ji[1], X. L. Ji[1], L. L. Jiang[1], L. W. Jiang[48], X. S. Jiang[1], J. B. Jiao[32], Z. Jiao[16], D. P. Jin[1], S. Jin[1], T. Johansson[47], A. Julin[41], N. Kalantar-Nayestanaki[24], X. L. Kang[1], X. S. Kang[29], M. Kavatsyuk[24], B. C. Ke[4], R. Kliemt[13], B. Kloss[21], O. B. Kolcu[38B,c], B. Kopf[3], M. Kornicer[40], W. Kuehn[23], A. Kupsc[47], W. Lai[1], J. S. Lange[23], M. Lara[18], P. Larin[13], Cheng Li[43], C. H. Li[1], D. M. Li[50], F. Li[1], G. Li[1], H. B. Li[1], J. C. Li[1], Jin Li[31], K. Li[12], K. Li[32], P. R. Li[39], T. Li[32], W. D. Li[1], W. G. Li[1], X. L. Li[32], X. M. Li[11], X. N. Li[1], X. Q. Li[29], Z. B. Li[36], H. Liang[43], Y. F. Liang[34], Y. T. Liang[23], G. R. Liao[10], D. X. Lin[13], B. J. Liu[1], C. L. Liu[4], C. X. Liu[1], F. H. Liu[33], Fang Liu[1], Feng Liu[5], H. B. Liu[11], H. H. Liu[1], H. H. Liu[15], H. M. Liu[1], J. Liu[1], J. P. Liu[48], J. Y. Liu[1], K. Liu[37], K. Y. Liu[26], L. D. Liu[30], Q. Liu[39], S. B. Liu[43], X. Liu[25], X. X. Liu[39], Y. B. Liu[29], Z. A. Liu[1], Zhiqiang Liu[1], Zhiqing Liu[21], H. Loehner[24], X. C. Lou[1,d], H. J. Lu[16], J. G. Lu[1], R. Q. Lu[17], Y. Lu[1], Y. P. Lu[1], C. L. Luo[27], M. X. Luo[49], T. Luo[40], X. L. Luo[1], M. Lv[1], X. R. Lyu[39], F. C. Ma[26], H. L. Ma[1], L. L. Ma[32], Q. M. Ma[1], S. Ma[1], T. Ma[1], X. N. Ma[29], X. Y. Ma[1], F. E. Maas[13], M. Maggiora[46A,46C], Q. A. Malik[45], Y. J. Mao[30], Z. P. Mao[1], S. Marcello[46A,46C], J. G. Messchendorp[24], J. Min[1], T. J. Min[1], R. E. Mitchell[18], X. H. Mo[1], Y. J. Mo[5], H. Moeini[24], C. Morales Morales[13], K. Moriya[18], N. Yu. Muchnoi[8,a], H. Muramatsu[41], Y. Nefedov[22], F. Nerling[13], I. B. Nikolaev[8,a], Z. Ning[1], S. Nisar[7], S. L. Niu[1], X. Y. Niu[1], S. L. Olsen[31], Q. Ouyang[1], S. Pacetti[19B], P. Patteri[19A], M. Pelizaeus[3], H. P. Peng[43], K. Peters[9], J. L. Ping[27], R. G. Ping[1], R. Poling[41], Y. N. Pu[17], M. Qi[28], S. Qian[1], C. F. Qiao[39], L. Q. Qin[32], N. Qin[48], X. S. Qin[1], Y. Qin[30], Z. H. Qin[1], J. F. Qiu[1], K. H. Rashid[45], C. F. Redmer[21], H. L. Ren[17], M. Ripka[21], G. Rong[1], X. D. Ruan[11], V. Santoro[20A], A. Sarantsev[22,e], M. Savrié[20B], K. Schoenning[47], S. Schumann[21], W. Shan[30], M. Shao[43], C. P. Shen[2], P. X. Shen[29], X. Y. Shen[1], H. Y. Sheng[1], M. R. Shepherd[18], W. M. Song[1], X. Y. Song[1], S. Sosio[46A,46C], S. Spataro[46A,46C], B. Spruck[23], G. X. Sun[1], J. F. Sun[14], S. S. Sun[1], Y. J. Sun[43], Y. Z. Sun[1], Z. J. Sun[1], Z. T. Sun[18], C. J. Tang[34], X. Tang[1], I. Tapan[38C], E. H. Thorndike[42], M. Tiemens[24], D. Toth[41], M. Ullrich[23], I. Uman[38B], G. S. Varner[40], B. Wang[29], B. L. Wang[39], D. Wang[30], D. Y. Wang[30], K. Wang[1], L. L. Wang[1], L. S. Wang[1], M. Wang[32], P. Wang[1], P. L. Wang[1], Q. J. Wang[1], S. G. Wang[30], W. Wang[1], X. F. Wang[37], Y. D. Wang[19A], Y. F. Wang[1], Y. Q. Wang[21], Z. Wang[1], Z. G. Wang[1], Z. H. Wang[43], Z. Y. Wang[1], D. H. Wei[10], J. B. Wei[30], P. Weidenkaff[21], S. P. Wen[1], U. Wiedner[3], M. Wolke[47], L. H. Wu[1], Z. Wu[1], L. G. Xia[37], Y. Xia[17], D. Xiao[1], Z. J. Xiao[27], Y. G. Xie[1], Q. L. Xiu[1], G. F. Xu[1], L. Xu[1], Q. J. Xu[12], Q. N. Xu[39], X. P. Xu[35], L. Yan[43], W. B. Yan[43], W. C. Yan[43], Y. H. Yan[17], H. X. Yang[1], L. Yang[48], Y. Yang[5], Y. X. Yang[10], H. Ye[1], M. Ye[1], M. H. Ye[6], J. H. Yin[1], B. X. Yu[1], C. X. Yu[29], H. W. Yu[30], J. S. Yu[25], C. Z. Yuan[1], W. L. Yuan[28], Y. Yuan[1], A. Yuncu[38B,f], A. A. Zafar[45], A. Zallo[19A], Y. Zeng[17], B. X. Zhang[1], B. Y. Zhang[1], C. Zhang[28], C. C. Zhang[1], D. H. Zhang[1], H. H. Zhang[36], H. Y. Zhang[1], J. J. Zhang[1], J. L. Zhang[1], J. Q. Zhang[1], J. W. Zhang[1], J. Y. Zhang[1], J. Z. Zhang[1], K. Zhang[1], L. Zhang[1], S. H. Zhang[1], X. J. Zhang[1], X. Y. Zhang[32], Y. Zhang[1], Y. H. Zhang[1], Z. H. Zhang[5], Z. P. Zhang[43], Z. Y. Zhang[48], G. Zhao[1], J. W. Zhao[1], J. Y. Zhao[1], J. Z. Zhao[1], Lei Zhao[43], Ling Zhao[1], M. G. Zhao[29], Q. Zhao[1], Q. W. Zhao[1], S. J. Zhao[50], T. C. Zhao[1], Y. B. Zhao[1], Z. G. Zhao[43], A. Zhemchugov[22,g], B. Zheng[44], J. P. Zheng[1], W. J. Zheng[32], Y. H. Zheng[39], B. Zhong[27], L. Zhou[1], Li Zhou[29], X. Zhou[48], X. K. Zhou[43], X. R. Zhou[43], X. Y. Zhou[1], K. Zhu[1], K. J. Zhu[1], S. Zhu[1], X. L. Zhu[37], Y. C. Zhu[43], Y. S. Zhu[1], Z. A. Zhu[1], J. Zhuang[1], B. S. Zou[1], J. H. Zou[1]

(BESIII Collaboration)

[1] Institute of High Energy Physics, Beijing 100049, People's Republic of China
[2] Beihang University, Beijing 100191, People's Republic of China
[3] Bochum Ruhr-University, D-44780 Bochum, Germany
[4] Carnegie Mellon University, Pittsburgh, Pennsylvania 15213, USA
[5] Central China Normal University, Wuhan 430079, People's Republic of China
[6] China Center of Advanced Science and Technology, Beijing 100190, People's Republic of China
[7] COMSATS Institute of Information Technology, Lahore, Defence Road, Off Raiwind Road, 54000 Lahore, Pakistan
[8] G.I. Budker Institute of Nuclear Physics SB RAS (BINP), Novosibirsk 630090, Russia
[9] GSI Helmholtzcentre for Heavy Ion Research GmbH, D-64291 Darmstadt, Germany
[10] Guangxi Normal University, Guilin 541004, People's Republic of China
[11] GuangXi University, Nanning 530004, People's Republic of China
[12] Hangzhou Normal University, Hangzhou 310036, People's Republic of China
[13] Helmholtz Institute Mainz, Johann-Joachim-Becher-Weg 45, D-55099 Mainz, Germany
[14] Henan Normal University, Xinxiang 453007, People's Republic of China

Typeset by REVTeX

[15] *Henan University of Science and Technology, Luoyang 471003, People's Republic of China*
[16] *Huangshan College, Huangshan 245000, People's Republic of China*
[17] *Hunan University, Changsha 410082, People's Republic of China*
[18] *Indiana University, Bloomington, Indiana 47405, USA*
[19] *(A)INFN Laboratori Nazionali di Frascati, I-00044, Frascati, Italy; (B)INFN and University of Perugia, I-06100, Perugia, Italy*
[20] *(A)INFN Sezione di Ferrara, I-44122, Ferrara, Italy; (B)University of Ferrara, I-44122, Ferrara, Italy*
[21] *Johannes Gutenberg University of Mainz, Johann-Joachim-Becher-Weg 45, D-55099 Mainz, Germany*
[22] *Joint Institute for Nuclear Research, 141980 Dubna, Moscow region, Russia*
[23] *Justus Liebig University Giessen, II. Physikalisches Institut, Heinrich-Buff-Ring 16, D-35392 Giessen, Germany*
[24] *KVI-CART, University of Groningen, NL-9747 AA Groningen, The Netherlands*
[25] *Lanzhou University, Lanzhou 730000, People's Republic of China*
[26] *Liaoning University, Shenyang 110036, People's Republic of China*
[27] *Nanjing Normal University, Nanjing 210023, People's Republic of China*
[28] *Nanjing University, Nanjing 210093, People's Republic of China*
[29] *Nankai University, Tianjin 300071, People's Republic of China*
[30] *Peking University, Beijing 100871, People's Republic of China*
[31] *Seoul National University, Seoul, 151-747 Korea*
[32] *Shandong University, Jinan 250100, People's Republic of China*
[33] *Shanxi University, Taiyuan 030006, People's Republic of China*
[34] *Sichuan University, Chengdu 610064, People's Republic of China*
[35] *Soochow University, Suzhou 215006, People's Republic of China*
[36] *Sun Yat-Sen University, Guangzhou 510275, People's Republic of China*
[37] *Tsinghua University, Beijing 100084, People's Republic of China*
[38] *(A)Ankara University, Dogol Caddesi, 06100 Tandogan, Ankara, Turkey; (B)Dogus University, 34722 Istanbul, Turkey; (C)Uludag University, 16059 Bursa, Turkey*
[39] *University of Chinese Academy of Sciences, Beijing 100049, People's Republic of China*
[40] *University of Hawaii, Honolulu, Hawaii 96822, USA*
[41] *University of Minnesota, Minneapolis, Minnesota 55455, USA*
[42] *University of Rochester, Rochester, New York 14627, USA*
[43] *University of Science and Technology of China, Hefei 230026, People's Republic of China*
[44] *University of South China, Hengyang 421001, People's Republic of China*
[45] *University of the Punjab, Lahore-54590, Pakistan*
[46] *(A)University of Turin, I-10125, Turin, Italy; (B)University of Eastern Piedmont, I-15121, Alessandria, Italy; (C)INFN, I-10125, Turin, Italy*
[47] *Uppsala University, Box 516, SE-75120 Uppsala, Sweden*
[48] *Wuhan University, Wuhan 430072, People's Republic of China*
[49] *Zhejiang University, Hangzhou 310027, People's Republic of China*
[50] *Zhengzhou University, Zhengzhou 450001, People's Republic of China*

[a] *Also at the Novosibirsk State University, Novosibirsk, 630090, Russia*
[b] *Also at the Moscow Institute of Physics and Technology, Moscow 141700, Russia and at the Functional Electronics Laboratory, Tomsk State University, Tomsk, 634050, Russia*
[c] *Currently at Istanbul Arel University, Kucukcekmece, Istanbul, Turkey*
[d] *Also at University of Texas at Dallas, Richardson, Texas 75083, USA*
[e] *Also at the PNPI, Gatchina 188300, Russia*
[f] *Also at Bogazici University, 34342 Istanbul, Turkey*
[g] *Also at the Moscow Institute of Physics and Technology, Moscow 141700, Russia*

Based on data samples collected with the BESIII detector at the BEPCII collider at 9 center-of-mass energies from 4.21 to 4.42 GeV, we search for the production of $e^+e^- \to \omega\chi_{cJ}$ ($J = 0, 1, 2$). The process $e^+e^- \to \omega\chi_{c0}$ is observed for the first time, and the Born cross sections at $\sqrt{s} = 4.23$ and 4.26 GeV are measured to be $(55.4 \pm 6.0 \pm 5.9)$ and $(23.7 \pm 5.3 \pm 3.5)$ pb, respectively, where the first uncertainties are statistical and the second are systematic. The $\omega\chi_{c0}$ signals at the other 7 energies and $e^+e^- \to \omega\chi_{c1}$ and $\omega\chi_{c2}$ signals are not significant, and the upper limits on the cross sections are determined. By examining the $\omega\chi_{c0}$ cross section as a function of center-of-mass energy, we find that it is inconsistent with the line shape of the $Y(4260)$ observed in $e^+e^- \to \pi^+\pi^- J/\psi$. Assuming the $\omega\chi_{c0}$ signals come from a single resonance, we extract mass and width of the resonance to be $(4230 \pm 8 \pm 6)$ MeV/c^2 and $(38 \pm 12 \pm 2)$ MeV, respectively, and the statistical significance is more than 9σ.

The charmonium-like state $Y(4260)$ was first observed in its decay to $\pi^+\pi^- J/\psi$ [1], and its decays into $\pi^0\pi^0 J/\psi$ and $K^+K^- J/\psi$ were reported from a study of 12.6 pb^{-1} data collected at 4.26 GeV by the CLEO-c experiment [2]. Contrary to the hidden charm final states, the $Y(4260)$ were found to have small coupling to open charm decay modes [3], as well as to light hadron final states [4, 5]. Recently, charged charmoniumlike states $Z_c(3900)$ $[\pi^{\pm}J/\psi]$ [6–8], $Z_c(3885)$ $[(D\bar{D}^*)^{\pm}]$ [9], $Z_c(4020)$ $[(\pi h_c)]$ [10, 11], and $Z_c(4025)$ $[(D^*\bar{D}^*)^{\pm}]$ [12] were observed in e^+e^- data collected around $\sqrt{s} = 4.26$ GeV. These features suggest the existence of a complicated substructure of the $Y(4260) \to \pi^+\pi^- J/\psi$ as well as the nature of the $Y(4260)$ itself. Searches for new decay modes and measuring the line shape may provide information that is useful for understanding the nature of the $Y(4260)$.

Many theoretical models have been proposed to interpret the $Y(4260)$, $e.g.$, as a quark-gluon charmonium hybrid, a tetraquark state, a hadro-charmonium, or a hadronic molecule [13]. The authors of Ref. [14] predict a sizeable coupling between the $Y(4260)$ and the $\omega\chi_{c0}$ channel by considering the threshold effect of $\omega\chi_{c0}$ that plays a role in reducing the decay rates into open-charm channels. By adopting the spin rearrangement scheme in the heavy quark limit and the experimental information, Ref. [15] predicts the ratio of the decays $Y(4260) \to \omega\chi_{cJ}$ $(J = 0, 1, 2)$ to be $4:3:5$.

In this Letter, we report on the study of $e^+e^- \to \omega\chi_{cJ}$ $(J = 0, 1, 2)$ based on the e^+e^- annihilation data samples collected with the BESIII detector [16] at 9 center-of-mass energy points in the range $\sqrt{s} = 4.21 - 4.42$ GeV. In the analysis, the ω meson is reconstructed via its $\pi^+\pi^-\pi^0$ decay mode, the χ_{c0} state is via $\pi^+\pi^-$ and K^+K^- decays, and the $\chi_{c1,2}$ states are via $\chi_{c1,2} \to \gamma J/\psi$, $J/\psi \to \ell^+\ell^-$ $(\ell = e, \mu)$.

We select charged tracks, photon, and $\pi^0 \to \gamma\gamma$ candidates as described in Ref. [17]. A candidate event must have four tracks with zero net charge and at least one π^0 candidate; for the $e^+e^- \to \omega\chi_{c1,2}$ channels, an additional photon is required. The tracks with a momentum larger than 1 GeV/c are identified as originating from χ_{cJ}, lower momentum pions are interpreted as originating from ω decays. A 5C kinematic fit is performed to constrain the total four-momentum of all particles in the final states to that of the initial e^+e^- system, and $M_{\gamma\gamma}$ is constrained to m_{π^0}. If more than one candidate occurs in an event, the one with the smallest χ^2_{5C} of the kinematic fit is selected. For the channel $e^+e^- \to \omega\chi_{c0}$, the two tracks from the χ_{c0} are assumed to be $\pi^+\pi^-$ or K^+K^- pairs. If $\chi^2_{5C}(\pi^+\pi^-) < \chi^2_{5C}(K^+K^-)$, the event is identified as originating from the $\pi^+\pi^-$ mode, otherwise it is considered to be from the K^+K^- mode. χ^2_{5C} is required to be less than 100. For the J/ψ reconstruction, the charged particle with the energy deposition in ECL larger than 1 GeV is identified as e, otherwise it is μ.

The χ^2_{5C} for the $\omega\chi_{c1,2}$ candidate event is required to be less than 60.

The main sources of background after event selection are found to be $e^+e^- \to \omega\pi^+\pi^-(\omega K^+K^-)$, where the $\pi^+\pi^-(K^+K^-)$ are not from χ_{c0} decays. The scatter plots of the invariant mass of $\pi^+\pi^-\pi^0$ versus that of $\pi^+\pi^-$ or K^+K^- for data at $\sqrt{s} = 4.23$ and 4.26 GeV are shown in Fig. 1. Clear accumulations of events are seen around the intersections of the ω and χ_{c0} regions, which indicate $\omega\chi_{c0}$ signals. Signal candidates are required to be in the ω signal region [0.75, 0.81] GeV/c^2, The ω sideband is taken as [0.60, 0.72] GeV/c^2 to estimate the non-resonant background.
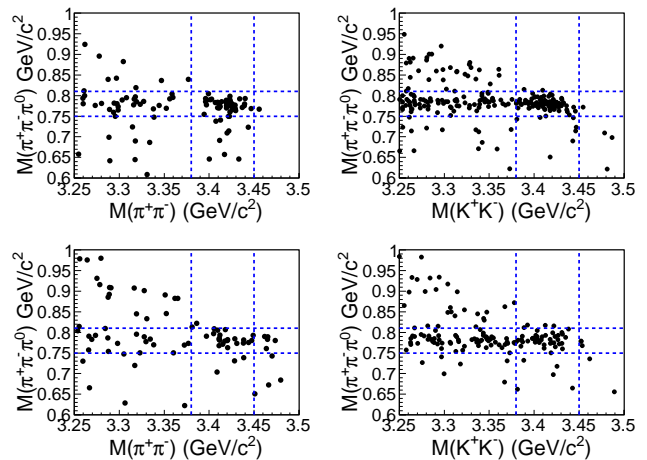

FIG. 1. Scatter plots of the $\pi^+\pi^-\pi^0$ invariant mass versus the $\pi^+\pi^-$ (left) and K^+K^- (right) invariant mass at $\sqrt{s} = 4.23$ GeV (top) and 4.26 GeV (bottom). The dashed lines denote the ω and χ_{c0} signal regions.

Figure 2 shows $M(\pi^+\pi^-)$ and $M(K^+K^-)$ at $\sqrt{s} = 4.23$ and 4.26 GeV after all requirements are imposed. To extract the signal yield, an unbinned maximum likelihood fit is performed on the $\pi^+\pi^-$ and K^+K^- modes simultaneously. The signal is described with a shape determined from the simulated signal MC sample. The background is described with an ARGUS function, $m\sqrt{1 - (m/m_0)^2} \cdot e^{k(1-(m/m_0)^2)}$ [18], where k is a free parameter in the fit, and m_0 is fixed at $\sqrt{s} - 0.75$ GeV (0.75 GeV is the lower limit of the $M(\pi^+\pi^-\pi^0)$ requirement). In the fit, the ratio of the number of $\pi^+\pi^-$ signal events to that of K^+K^- signal events is fixed to be $\frac{\epsilon_\pi \mathcal{B}(\chi_{c0} \to \pi^+\pi^-)}{\epsilon_K \mathcal{B}(\chi_{c0} \to K^+K^-)}$, where $\mathcal{B}(\chi_{c0} \to \pi^+\pi^-)$ and $\mathcal{B}(\chi_{c0} \to K^+K^-)$ are taken as world average values [19], and ϵ_π and ϵ_K are the efficiencies of $\pi^+\pi^-$ and K^+K^- modes determined from MC simulations, respectively. The possible interference between the signal and background is neglected. The fit results are shown in Fig. 2. For the $\sqrt{s} = 4.23$ GeV data, the total signal yield of the two modes is 125.3 ± 13.5, and the signal statistical significance is 11.9σ. By pro-

jecting the events of the two modes into two histograms (at least 7 events per bin), the goodness-of-fit is found to be χ^2/d.o.f. $= 37.6/22$, where the d.o.f. is the number of degrees of freedom. For the $\sqrt{s} = 4.26$ GeV data, the total signal yield is 45.5 ± 10.2 with a statistical significance of 5.5σ, and χ^2/d.o.f. $= 27.1/15$. Since the statistics at the other energy points are very limited, the number of the observed events is obtained by counting the entries in the χ_{c0} signal region [3.38, 3.45] GeV/c^2, and the number of background events in the signal region is obtained by fitting the $M(\pi^+\pi^-)$ $[M(K^+K^-)]$ spectrum excluding the χ_{c0} signal region and scaling to the size of the signal region.
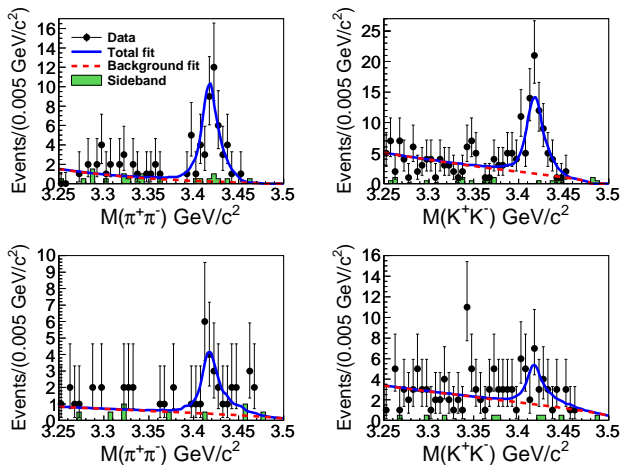
FIG. 2. Fit to the invariant mass distributions $M(\pi^+\pi^-)$ (left) and $M(K^+K^-)$ (right) after requiring $M(\pi^+\pi^-\pi^0)$ in the ω signal region at $\sqrt{s} = 4.23$ GeV (top) and 4.26 GeV (bottom). Points with error bars are data, the solid curves are the fit results, the dashed lines indicate the background and the shaded histograms show the normalized ω sideband events.

For the process $e^+e^- \to \omega\chi_{c1,2}$, the main remaining backgrounds stem from $e^+e^- \to \pi^+\pi^-\psi'$, $\psi' \to \pi^0\pi^0 J/\psi$ and $e^+e^- \to \pi^0\pi^0\psi'$, $\psi' \to \pi^+\pi^- J/\psi$. To suppress these backgrounds, we exclude events in which the invariant mass $M(\pi^+\pi^-\ell^+\ell^-)$ or the mass recoiling against $\pi^+\pi^-$ $[M^{\text{recoil}}(\pi^+\pi^-)]$ lie in the region [3.68, 3.70] GeV/c^2.

The J/ψ and ω signal regions are set to be [3.08, 3.12] GeV/c^2 and [0.75, 0.81] GeV/c^2, respectively. After all the requirements are applied, no obvious signals are observed at $\sqrt{s} = 4.31$, 4.36, 4.39, and 4.42 GeV. The number of observed events is obtained by counting events in the χ_{c1} or χ_{c2} signal regions, which are defined as [3.49, 3.53] or [3.54, 3.58] GeV/c^2, respectively. The number of background events in the signal regions is estimated with data obtained from the sideband region [3.35, 3.47] GeV/c^2 in the $M(\gamma J/\psi)$ distribution by assuming a flat distribution in the full mass range.

The Born cross section is calculated from

$$\sigma^{\text{B}} = \frac{N^{\text{obs}}}{\mathcal{L}(1+\delta^r)(1+\delta^v)(\epsilon_1\mathcal{B}_1 + \epsilon_2\mathcal{B}_2)\mathcal{B}_3}, \quad (1)$$

where N^{obs} is the number of observed signal events, $\mathcal{L}$ is the integrated luminosity, $(1 + \delta^r)$ is the radiative correction factor which is obtained by using a QED calculation [20] and taking the cross section measured in this analysis with two iterations as input, $(1 + \delta^v)$ is the vacuum polarization factor which is taken from a QED calculation [21]. For the $e^+e^- \to \omega\chi_{c0}$ $[\omega\chi_{c1,2}]$ channel, $\mathcal{B}_1 = \mathcal{B}(\chi_{c0} \to \pi^+\pi^-)$ $[\mathcal{B}(J/\psi \to e^+e^-)]$, $\mathcal{B}_2 = \mathcal{B}(\chi_{c0} \to K^+K^-)$ $[\mathcal{B}(J/\psi \to \mu^+\mu^-)]$, $\mathcal{B}_3 = \mathcal{B}(\omega \to \pi^+\pi^-\pi^0) \times \mathcal{B}(\pi^0 \to \gamma\gamma)$ $[\mathcal{B}(\chi_{c1,2} \to \gamma J/\psi) \times \mathcal{B}(\omega \to \pi^+\pi^-\pi^0) \times \mathcal{B}(\pi^0 \to \gamma\gamma)]$, and ϵ_1 and ϵ_2 are the efficiencies for the $\pi^+\pi^-$ $[e^+e^-]$ and K^+K^- $[\mu^+\mu^-]$ modes, respectively. For center of mass energies where the signal is not significant, we set upper limits at the 90% confidence level (C.L.) on the Born cross section [22]. The Born cross section or its upper limit at each energy point for $e^+e^- \to \omega\chi_{c0}$ and $e^+e^- \to \omega\chi_{c1,2}$ are listed in Tables I and II, respectively.

Figure 3 shows the measured Born cross sections for $e^+e^- \to \omega\chi_{c0}$ over the energy region studied in this work (we follow the convention to fit the dressed cross section $\sigma^{\text{B}} \cdot (1 + \delta^v)$ in extracting the resonant parameters in [19]). A maximum likelihood method is used to fit the shape of the cross section.

Assuming that the $\omega\chi_{c0}$ signals come from a single resonance, a phase-space modified Breit-Wigner (BW) function

$$\text{BW}(\sqrt{s}) = \frac{\Gamma_{ee}\mathcal{B}(\omega\chi_{c0})\Gamma_t}{(s-M^2)^2 + (M\Gamma_t)^2} \cdot \frac{\Phi(\sqrt{s})}{\Phi(M)} \quad (2)$$

is used to parameterize the resonance, where Γ_{ee} is the e^+e^- partial width, Γ_t the total width, and $\mathcal{B}(\omega\chi_{c0})$ the branching fraction of the resonance decay to $\omega\chi_{c0}$. $\Phi(\sqrt{s}) = \frac{P}{\sqrt{s}}$ is the phase space factor for an S-wave two-body system, where P is the ω momentum in the e^+e^- center-of-mass frame. We fit the data with a coherent sum of the BW function and a phase space term and find that the phase space term does not contribute significantly. The fit results for the resonance parameters are $\Gamma_{ee}\mathcal{B}(\omega\chi_{c0}) = (2.7 \pm 0.5)$ eV, $M = (4230 \pm 8)$ MeV/c^2, and $\Gamma_t = (38 \pm 12)$ MeV. Fitting the data using the only phase space term results in a large change of the likelihood $[\Delta(-2\ln L) = 101.6]$. Taking the change of 4 in the d.o.f.s into account, this corresponds to a statistical significance of $> 9\sigma$.

The systematic uncertainties in the Born cross section measurement mainly originate from the radiative correction, the luminosity measurement, the detection efficiency, and the kinematic fit. A 10% uncertainty of in the radiative correction is estimated by varying the line shape of the cross section in the generator from the

TABLE I. The results on $e^+e^- \to \omega\chi_{c0}$. Shown in the table are the integrated luminosity $\mathcal{L}$, product of radiative correction factor, branching fraction and efficiency $\mathcal{D} = (1+\delta^r) \cdot (\epsilon_\pi \cdot \mathcal{B}(\chi_{c0} \to \pi^+\pi^-) + \epsilon_K \cdot \mathcal{B}(\chi_{c0} \to K^+K^-))$, number of observed events N^{obs} (the numbers of background are subtracted at $\sqrt{s} = 4.23$ and 4.26 GeV), number of estimated background N^{bkg}, vacuum polarization factor $(1+\delta^v)$, Born cross section σ^{B}, and upper limit (at the 90% C.L.) on Born cross section $\sigma_{\mathrm{UL}}^{\mathrm{B}}$ at each energy point. The first uncertainty of the Born cross section is statistical, and the second systematic. The dashes mean not available.

$\sqrt{s}$ (GeV)	$\mathcal{L}$ (pb^{-1})	$\mathcal{D}$ ($\times 10^{-3}$)	N^{obs}	N^{bkg}	$1+\delta^v$	σ^{B} (pb)	$\sigma_{\mathrm{UL}}^{\mathrm{B}}$ (pb)
4.21	54.6	1.99	7	5.0 ± 2.8	1.057	$20.2^{+46.3}_{-37.7} \pm 3.3$	< 90
4.22	54.1	2.12	7	4.3 ± 2.1	1.057	$25.1^{+39.4}_{-30.4} \pm 2.0$	< 81
4.23	1047.3	2.29	125.3 ± 13.5	-	1.056	$55.4 \pm 6.0 \pm 5.9$	-
4.245	55.6	2.44	6	4.0 ± 1.5	1.056	$16.3^{+30.8}_{-22.3} \pm 1.5$	< 60
4.26	826.7	2.50	45.5 ± 10.2	-	1.054	$23.7 \pm 5.3 \pm 3.5$	-
4.31	44.9	2.56	5	2.2 ± 1.6	1.053	$26.2^{+34.9}_{-25.1} \pm 2.2$	< 76
4.36	539.8	2.62	29	32.4 ± 4.7	1.051	$-2.6^{+6.1}_{-5.4} \pm 0.27$	< 6
4.39	55.2	2.57	2	0.6 ± 0.7	1.051	$10.4^{+20.7}_{-11.2} \pm 0.7$	< 37
4.42	44.7	2.46	0	1.4 ± 1.5	1.053	$-13.6^{+18.5}_{-14.7} \pm 1.3$	< 15

TABLE II. The results on $e^+e^- \to \omega\chi_{c1,2}$. Listed in the table are the product of radiative correction factor, branching fraction and efficiency $\mathcal{D} = (1+\delta^r) \cdot (\epsilon_e \cdot \mathcal{B}(J/\psi \to e^+e^-) + \epsilon_\mu \cdot \mathcal{B}(J/\psi \to \mu^+\mu^-))$, number of the observed events N^{obs}, number of backgrounds N^{bkg} in sideband regions, and the upper limit (at the 90% C.L.) on the Born cross section $\sigma_{\mathrm{UL}}^{\mathrm{B}}$.

Mode	$\sqrt{s}$ (GeV)	$\mathcal{D}$ ($\times 10^{-2}$)	N^{obs}	N^{bkg}	$\sigma_{\mathrm{UL}}^{\mathrm{B}}$ (pb)
$\omega\chi_{c1}$	4.31	1.43	1	$0.0^{+1.2}_{-0.0}$	< 18
	4.36	1.27	1	$1.0^{+2.3}_{-0.8}$	< 0.9
	4.39	1.27	1	$0.0^{+1.2}_{-0.0}$	< 17
	4.42	1.25	0	$0.0^{+1.2}_{-0.0}$	< 11
$\omega\chi_{c2}$	4.36	0.95	5	$1.0^{+2.3}_{-0.8}$	< 11
	4.39	1.06	3	$0.0^{+1.2}_{-0.0}$	< 64
	4.42	0.98	2	$0.0^{+1.2}_{-0.0}$	< 61

FIG. 3. Fit to $\sigma(e^+e^- \to \omega\chi_{c0})$ with a resonance (solid curve), or a phase space term (dot-dashed curve). Dots with error bars are the dressed cross sections. The uncertainties are statistical only.

measured energy-dependent cross section to the $Y(4260)$ BW shape. Due to the limitation of the statistics, this item imports the biggest uncertainty. The polar angle θ of the ω in the e^+e^- center-of-mass frame is defined as the angle between ω and e^- beam. For the $\omega\chi_{c0}$ channel, the distribution of θ is obtained from data taken at 4.23 GeV and fitted with $1 + \alpha\cos^2\theta$. The value of α is determined to be -0.28 ± 0.31. The efficiencies are determined from MC simulations, and the uncertainty is estimated by varying α within one standard deviation. For the $\omega\chi_{c1,2}$ channels, a 1% uncertainty is estimated by varying the ω angular distribution from flat to $1 \pm \cos^2\theta$. The uncertainty of luminosity is 1%. The uncertainty in tracking efficiency is 1% per track. The uncertainty in photon reconstruction is 1% per photon. A 1% uncertainty in the kinematic fit is estimated by correcting the helix parameters of charged tracks [24].

For the $e^+e^- \to \omega\chi_{c0}$ mode, additional uncertainties come from the cross feed between K^+K^- and $\pi^+\pi^-$ modes, and the fitting procedure. The uncertainty due to the cross feed is estimated to be 1% by using the signal MC samples. A 4% uncertainty from the fitting range
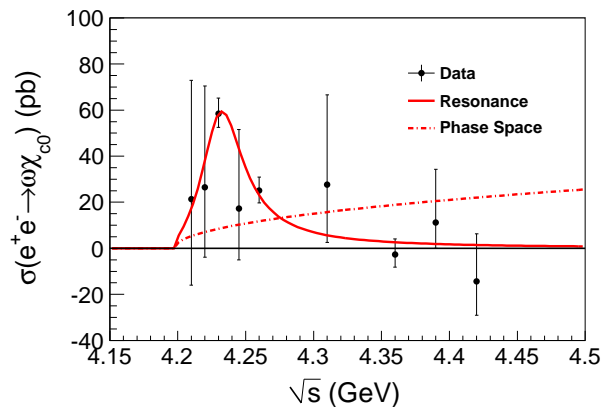
is obtained by varying the limits of the fitting range by ± 0.05 GeV/c^2. The uncertainty from the mass resolution is determined to be negligible compared to the resolutions of the reconstructed ω in data and MC samples. The uncertainties associated with $\mathcal{B}(\chi_{c0} \to \pi^+\pi^-)$ and $\mathcal{B}(\chi_{c0} \to K^+K^-)$ are obtained to be 4% by varying the branching fractions around their world average values by one standard deviation [19]. A 5% uncertainty due to the choice of the background shape is estimated by changing the background shape from the ARGUS function to a second order polynomial (where the parameters of the polynomial are allowed to float). The overall systematic errors are obtained by summing all the sources of systematic uncertainties in quadrature by assuming they are independent. For the $\omega\chi_{c0}$ channel, they vary from 6.7% to 16.1% depending on the center of mass energies.

The systematic uncertainties on the resonant parameters in the fit to the energy-dependent cross section of $e^+e^- \to \omega\chi_{c0}$ are mainly from the uncertainties of $\sqrt{s}$ de-

termination, energy spread, parametrization of the BW function, and the cross section measurement. A precision of 2 MeV [25] of the center-of-mass energy introduce a ± 2 MeV/c^2 uncertainty in the mass measurement. To estimate the uncertainty from the energy spread of $\sqrt{s}$ (1.6 MeV), a BW function convoluted with a Gaussian function with a resolution of 1.6 MeV is used to fit the data, and the uncertainties are estimated by comparing the results with the nominal ones. Instead of using a constant total width, we assume a mass dependent width $\Gamma_t = \Gamma_t^0 \cdot \frac{\Phi(\sqrt{s})}{\Phi(M)}$, where Γ_t^0 is the width of the resonance, to estimate the systematic uncertainty due to signal parametrization. The systematic uncertainty of the Born cross section (except that from $1 + \delta^v$) contributes uncertainty in $\Gamma_{ee}\mathcal{B}(\omega\chi_{c0})$. By adding all these sources of systematic uncertainties in quadrature, we obtain uncertainties of ± 6 MeV/c^2, ± 2 MeV, and ± 0.4 eV for the mass, width, and the partial width, respectively.

In summary, based on data samples collected between $\sqrt{s} = 4.21$ and 4.42 GeV collected with the BESIII detector, the process $e^+e^- \rightarrow \omega\chi_{c0}$ is observed at $\sqrt{s} = 4.23$ and 4.26 GeV for the first time, and the Born cross sections are measured to be $(55.4 \pm 6.0 \pm 5.9)$ and $(23.7 \pm 5.3 \pm 3.5)$ pb, respectively. For other energy points, no significant signals are found and upper limits on the cross section at the 90% C.L. are determined. The data reveals a sizeable $\omega\chi_{c0}$ production around 4.23 GeV/c^2 as predicted in Ref. [14]. By assuming the $\omega\chi_{c0}$ signals come from a single resonance, we extract the $\Gamma_{ee}\mathcal{B}(\omega\chi_{c0})$, mass, and width of the resonance to be $(2.7 \pm 0.5 \pm 0.4)$ eV, $(4230 \pm 8 \pm 6)$ MeV/c^2, and $(38 \pm 12 \pm 2)$ MeV, respectively. The parameters are inconsistent with those obtained by fitting a single resonance to the $\pi^+\pi^- J/\psi$ cross section [1]. This suggests that the observed $\omega\chi_{c0}$ signals be unlikely to originate from the $Y(4260)$. The $e^+e^- \rightarrow \omega\chi_{c1,2}$ channels are also sought for, but no significant signals are observed; upper limits at the 90% C.L. on the production cross sections are determined. The very small measured ratios of $e^+e^- \rightarrow \omega\chi_{c1,2}$ cross sections to those for $e^+e^- \rightarrow \omega\chi_{c0}$ are inconsistent with the prediction in Ref. [15].

[1] B. Aubert *et al.* [BaBar Collaboration], Phys. Rev. Lett. **95**, 142001 (2005).

[2] T. E. Coan *et al.* [CLEO Collboration], Phys. Rev. Lett. **96**, 162003 (2006).

[3] G. Pakhlova *et al.* [Belle Collaboration], Phys. Rev. Lett. **98**, 092001 (2007).

[4] B. Aubert *et al.* [BaBar Collaboration], Phys. Rev. D **77**, 092002 (2008).

[5] B. Aubert *et al.* [BaBar Collaboration], Phys. Rev. D **74**, 091103 (2006).

[6] M. Ablikim *et al.* [BESIII Collaboration], Phys. Rev. Lett. **110**, 252001 (2013).

[7] Z. Q. Liu *et al.* [Belle Collaboration], Phys. Rev. Lett. **110**, 252002 (2013).

[8] T. Xiao, S. Dobbs, A. Tomaradze and K. K. Seth, Phys. Lett. B **727**, 366 (2013).

[9] M. Ablikim *et al.* [BESIII Collaboration], Phys. Rev. Lett. **112**, 022001 (2014).

[10] M. Ablikim *et al.* [BESIII Collaboration], Phys. Rev. Lett. **111**, 242001 (2013).

[11] M. Ablikim *et al.* [BESIII Collaboration], arXiv:1409.6577.

[12] M. Ablikim *et al.* [BESIII Collaboration], Phys. Rev. Lett. **112**, 132001 (2014).

[13] N. Brambilla *et al.* [Quarkonium Working Group], Eur. Phys. J. C **71**, 1534 (2011).

[14] L. Y. Dai, M. Shi, G. Y. Tang, H. Q. Zheng, arXiv:1206.6911v2.

[15] L. Ma, X. H. Liu, X. Liu, S. L. Zhu, arXiv:1406.6879.

[16] M. Ablikim *et al.* [BESIII Collaboration], Nucl. Instrum. Meth. A **614**, 345 (2010).

[17] M. Ablikim *et al.* [BESIII Collaboration], Phys. Rev. Lett. **104**, 132002 (2011).

[18] H. Albrecht *et al.* [ARGUS Collaboration], Phys. Lett. B **241**, 278 (1990).

[19] J. Beringer *et al.* [Particle Data Group], Phys. Rev D **86**, 010001 (2012).

[20] E. A. Kuraev and V. S. Fadin, Sov. J. Nucl. Phys. **41**, 466 (1985) [Yad. Fiz. **41**, 733 (1985)].

[21] S. Actis *et al.* Eur. Phys. J. C **66**, 585 (2010).

[22] The upper limit is calculated by using a frequentist method with unbounded profile likelihood treatment of systematic uncertainties, which is implemented by a C++ class TROLKE in the ROOT framework [23]. The number of the observed events is assumed to follow a Poisson distribution, the number of background events

and the efficiency are assumed to follow Gaussian distributions. In order to consider the systematic uncertainty in the calculation, we use the denominator in Eq. (1) as an effective efficiency as implemented in TROLKE.

[23] W. A. Rolke, A. M. Lopez and J. Conrad, Nucl. Instr. Meth. A **551**, 493 (2005).

[24] M. Ablikim *et al.* [BESIII Collaboration], Phys. Rev. D **87**, 012002 (2013).

[25] E. V. Abakumova, *et al.*, Nucl. Instrum. Meth. A **659**, 21 (2011).